small
NANO MICRO

Optically Induced Cell Fusion Using Bispecific Nanoparticles

Daniella Yeheskely-Hayon, Limor Minai, Lior Golan, Eldad J. Dann, and Dvir Yelin*

***R**edirecting the immune system to eliminate tumor cells is a promising alternative to traditional cancer therapies, most often requiring direct interaction between an immune system effector cell and its target. Herein, a novel approach for selective attachment of malignant cells to antigen-presenting cells by using bispecific nanoparticles is presented. The engaged cell pairs are then irradiated by a sequence of resonant femtosecond pulses, which results in widespread cell fusion and the consequent formation of hybrid cells. The dual role of gold nanoparticles as conjugating agents and fusion promoters offers a simple yet effective means for specific fusion between different cells. This technology could be useful for a variety of in vitro and in vivo applications that call for selective fusion between cells within a large heterogenic cell population.*

1. Introduction

Physical contact between cells is a key step toward the establishment of various signal transduction pathways that take part in the complex intercellular communication system. An important example is the interaction between immune system effector cells and foreign cells, which involves cell attachment, specific recognition, and the execution of various mechanisms for destroying the foreign cell.[1] Today, redirecting the immune system for the purpose of cancer cell elimination is a promising alternative to traditional therapies; various techniques have been studied in an attempt to promote attachment between tumor cells and cytotoxic T lymphocytes (CTLs)[2] or natural killer (NK) cells.[3] Coupling between the different cell types is often achieved by using bispecific antibodies, i.e., molecules that possess high affinity to receptors on two different cell types. Bispecific antibodies were initially produced by chemical linkage[4,5] or heterohybridoma,[6] and were shown to successfully bind malignant cells to CTLs,[7,8] macrophages,[9] and NK cells;[10] however, such complex molecules are often difficult to synthesize and may have poor chemical stability.[11] In the last decade, advanced molecular engineering approaches have enabled the use of new and improved bispecific molecules,[12,13] which address some of the difficulties faced by previous methods by improving stability and potency.

Recent studies have shown that dendritic cells (DCs) fused to primary tumor cells[14] from patients with ovarian carcinoma,[15] breast carcinoma,[16] malignant glioma,[17] leukemia,[18]and multiple myeloma[19] have stimulated strong CTL activity against autologous tumor cells.[20,21] The integration of the cytoplasm from a tumor cell into the DC may facilitate the entry of tumor antigens into the DC's antigen processing and presenting pathway.[22] Cell fusion for these applications most often involves the use of polyethylene glycol (PEG),[23] which replaces the water molecules in contact with the plasma membrane and compromises its integrity. Although this method is relatively straightforward, it often suffers from low efficiency and high toxicity.[24,25] Additional methods for promoting cell fusion involve the use of electroporation[26] and viruses.[27] The use of a tightly focused femtosecond laser beam[28] has also been proposed

Dr. D. Yeheskely-Hayon, Dr. L. Minai, L. Golan, Prof. D. Yelin
Department of Biomedical Engineering
Technion-Israel Institute of Technology
32000 Haifa, Israel
E-mail: danih@bm.technion.ac.il
Prof. E. J. Dann
Department of Hematology and Bone Marrow Transplantation
Blood Bank and Aphaeresis Unit
Rambam Medical Center and Bruce Rappaport Faculty of Medicine
Technion-Israel Institute of Technology
31096 Haifa, Israel

DOI: 10.1002/smll.201300696

for promoting fusion between neighboring cells by rupturing their membranes at specific locations.[29,30] None of these methods, however, is selective to specific types of cells, thus preventing their potential use for in vivo therapy or for other applications in which prior cell sorting or isolation is challenging or impractical.

Herein, we present a novel approach for specifically engaging and fusing selected cells by using custom-designed, bispecific nanoparticles and subsequent irradiation by a tailored sequence of resonant femtosecond pulses. Our bispecific nanoparticle comprises a gold sphere coated by a layer containing two different antibodies having high affinity to two target cells. The nanoparticles play a dual role in promoting fusion: first, their dual affinity to both the tumor cells and the immune system cells effectively binds these cells together; second, their unique optical properties at resonance irradiation conditions allow intense laser pulses to locally compromise the cells' membranes. By using this technique, we demonstrate efficient selective coupling between malignant B cells and antigen-presenting cells, followed by successful fusion triggered by the irradiation of a few intense laser pulses.

2. Results

2.1. Specific Attachment Using Dual-Affinity Gold Nanoparticles

The abundance of well-defined clusters of differentiation antigens CD20[31] and CD86[32] was detected by using flow cytometry of Burkitt lymphoma B (BJAB) cells and human monocyte-derived DCs, respectively (**Figure 1**a). A schematic illustration of the structure of a nanoparticle having affinity to both of these cells is shown in Figure 1b. The bispecific nanoparticles are obtained by mixing 25-nm-diameter gold spheres with equal amounts of chimeric CD20 monoclonal antibody (Rituximab) and human CD86 antibody, using *o*-pyridyldisulfide-PEG-*n*-hydroxylsuccinimide (OPSS-PEG-NHS; 2000 kDa) as a linker between the antibodies and the gold surface. Conjugation of both antibodies to the gold particles was confirmed (Figure 1c) by gel electrophoresis followed by Western blot analysis, in which the antibodies were removed from the particles and analyzed using specific antibodies.

The attachment between two different cells via a bispecific nanoparticle is illustrated in **Figure 2**a. Following the addition of the nanoparticles to the growth medium of an equally (1:1) mixed BJAB (green labeled) and human monocyte-derived dendritic (blue labeled) cell population (Figure 2b), approximately 30% of the cells formed pairs or small clusters of physically attached cells (Figure 2c). Significantly lower cell attachment levels of 7, 6.5, and 4.5% were observed when incubating similar cell mixtures with only single antibody (anti-CD20) nanoparticles, nonspecific anti-epidermal growth factor receptor (EGFR)-coated nanoparticles, and in the absence of nanoparticles, respectively.

A closer view of a fixated BJAB–DC pair is shown in the false-color scanning electron microscopy (SEM) image (**Figure 3**a), revealing the light-toned BJAB cell (green) attached to the larger and feature-rich DC (blue). A magnified view (Figure 3b) of the region marked by a rectangle in Figure 3a, overlaid by an atomic-number-sensitive image of the same field of view, reveals a relatively uniform distribution of the individual gold nanoparticles (orange-yellow) on the plasma membranes of both cells, without any noticeable particle aggregation. Based on these images, we estimate particle densities of approximately 40 and 12 particles μm^{-2} on the BJAB and the DCs, respectively. As expected, due to the presence of numerous identical antibodies on each particle, attachment between cells of a similar type after incubation with bispecific nanoparticles was also evident: more than 40% of the BJAB cells and approximately 2% of DCs appeared as part of small (2–10 cells) clusters.

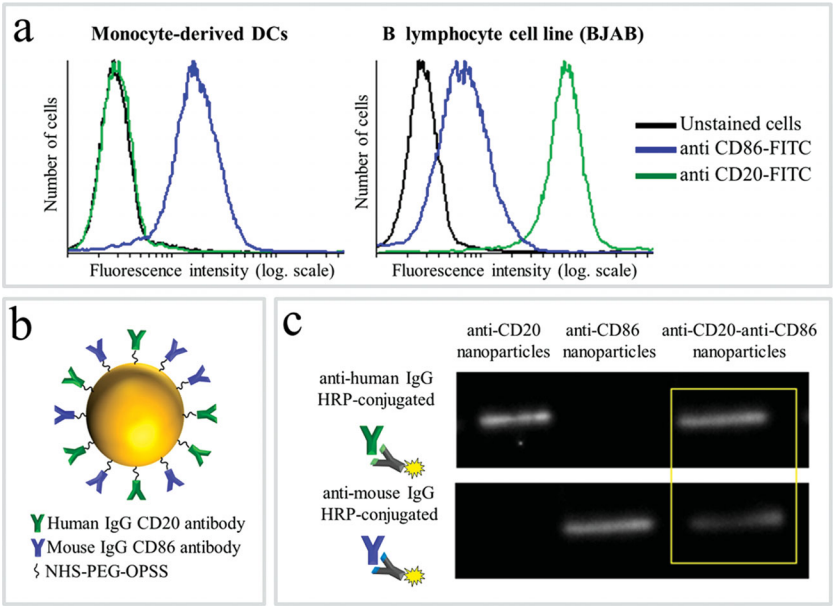

Figure 1. Bispecific nanoparticles. a) Flow cytometry histograms representing fluorescence (secondary fluorescein isothiocyanate (FITC)-conjugated antibody) intensity of dendritic and BJAB cells incubated with anti-CD86 (blue curves) and anti-CD20 (green curves). b) Schematic of a bispecific anti-CD20–anti-CD86 gold nanoparticle. c) Western blot analysis of the coating molecules of the bispecific nanoparticles, showing the presence of both antibodies on the particles. IgG=immunoglobulin G, HRP=horseradish peroxidase.

2.2. Optically Induced Fusion between Engaged Cells

Cells engaged in a physical contact do not normally fuse together in the absence of specific biological or chemical induction signals. Consequently, spontaneous fusion events were not observed at any of the cell cultures even after several hours. In a previous work[33] we have shown that cells within a homogeneous solution incubated with monospecific (single antibody

small 2013,
DOI: 10.1002/smll.201300696

NANO MICRO small

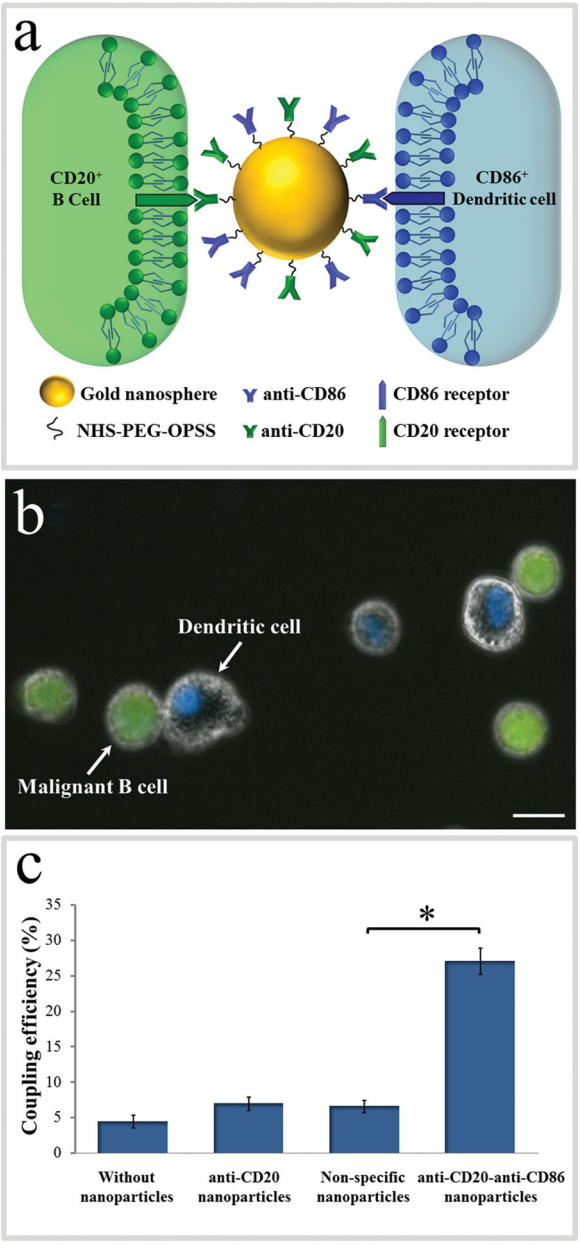

Figure 2. Cell coupling using a bispecific nanoparticle. a) Schematic illustration of nanoparticle-mediated coupling between a malignant B cell and a DC. b) Fluorescence-phase contrast image of BJAB cells (green cytoplasm) attached to DCs (blue nuclei). Scale bar represents 10 µm. c) Cell attachment efficiency using different nanoparticles. (*) indicates $P < 0.0001$.

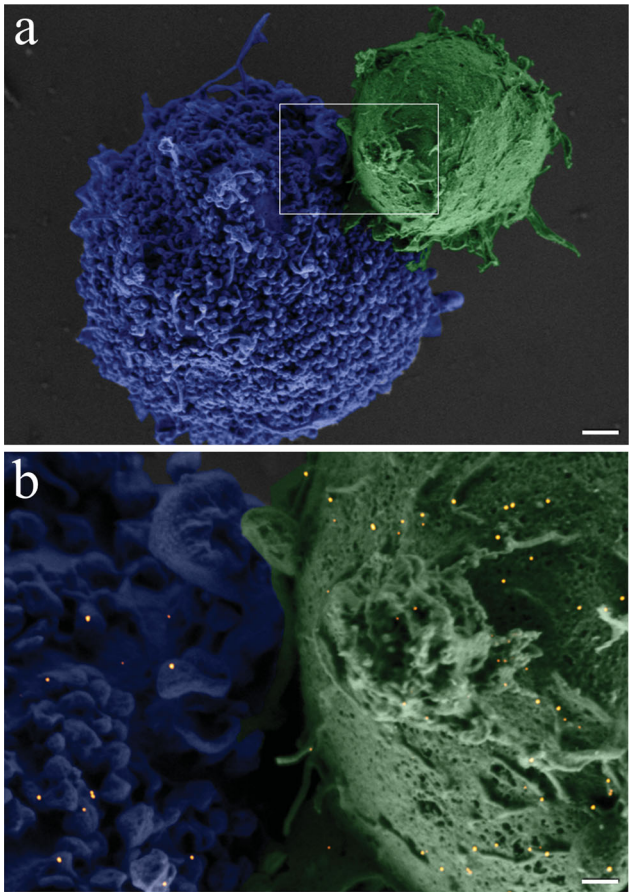

Figure 3. Bispecific gold nanoparticles on the plasma membrane of a coupled BJAB–DC pair. a) SEM image of the dendritic (false color blue) and BJAB (false color green) cell pair. Scale bar represents 1 µm. b) Magnified view of the region marked by a rectangle in (a), overlaid by a back-scattering detection image that reveals the presence of gold nanoparticles (false color yellow). Scale bar represents 200 nm.

coating) gold nanospheres were led to fuse following irradiation by a few high-intensity femtosecond pulses that were tuned to the plasmonic resonance wavelength of the nanoparticles. The fusion efficiency of cells of different types was extremely low in these experiments due to the random and transient physical contacts between the cells.

To demonstrate specific cell fusion, the entire volume of the culture containing the coupled BJAB–DC pairs was washed off the unbound nanoparticles and irradiated by a sequence (ten pulses, 1 kHz repetition rate) of intense (12 mJ cm^{-2}), ultrashort (50 fs), resonant (545 nm wavelength) laser pulses. Time-lapse fluorescence-phase contrast imaging of two exemplary fusion events between BJAB and DCs is shown in **Figure 4**a. Data analysis based on 1000 cells revealed that fusion between BJAB and DCs was less common (7%) than fusion between homogeneous pairs (or clusters) of BJAB cells only (20%). Moreover, DC–DC fusion was not detected at all, unless a BJAB cell was involved in the fusion process into a DC–DC–BJAB cell hybrid. The irradiated BJAB cells and DCs that were in physical contact showed first signs of morphological changes immediately after irradiation, toward the formation of hybrid cells with a unified cytoplasm after 20–30 min (Figure 4a). A schematic model of the fusion process between engaged cells irradiated by femtosecond pulses is illustrated in Figure 4b, which depicts the local disruption of the cells' plasma membranes initiated by the several tens of nanometers in diameter[34,35] cavitation bubble that has been formed around the particle.[36]

In addition to DCs, foreign or tumor antigens could also be presented to the adaptive immune system by macrophages, following attachment and fusion with the target cells. To demonstrate the induction of fusion between macrophages and malignant B cells, monocyte-derived macrophages expressing

DOI: 10.1002/smll.201300696

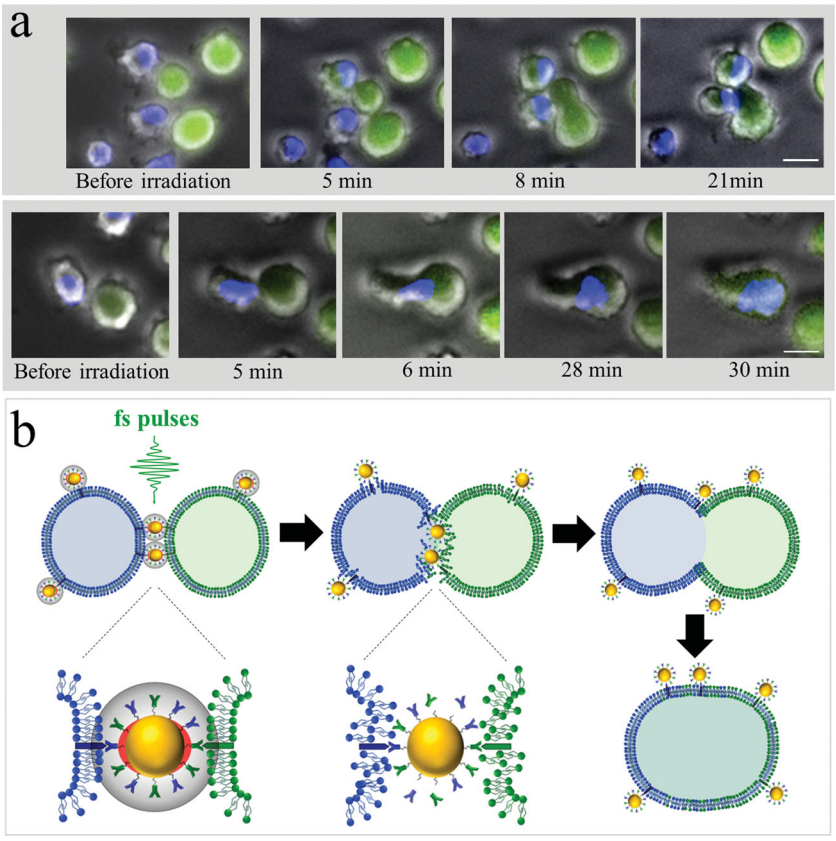

Figure 4. Fusion between dendritic and BJAB cells. a) Two time sequences of fluorescence-phase contrast images of fusing BJAB cells (green cytoplasm) and DCs (blue nuclei) following incubation with anti-CD20–anti-CD86 nanoparticles and irradiation by ten pulses. Scale bars represent 10 μm. b) Schematic illustration of the fusion process between attached cells triggered by femtosecond pulses.

CD86 surface receptors were mixed with CD20-expressing BJAB cells and incubated within a medium containing bispecific anti-CD20–anti-CD86 nanoparticles. After 15 min of incubation, nearly 50% of the macrophages in the culture were found attached to BJAB cells (**Figure 5**a,b), a significantly higher rate compared with coupling in a nanoparticle-free medium (20%). In contrast, the use of monospecific anti-CD86 nanoparticles resulted in 26% macrophage–BJAB cell attachment and 30% macrophage–macrophage attachment. After irradiation by a single sequence (ten pulses, 1 kHz repetition rate) of femtosecond pulses, approximately 9% of the macrophage–BJAB cell pairs were successfully fused. A typical fusing pair of cells is shown in a time-lapse image sequence in Figure 5c, which reveals the plasma membrane fusion (phase contrast, top row), cytoplasmic (green fluorescence, second row) transfer from the BJAB cell during fusion, and gradual passage of the nuclear blue marker from the macrophage nucleus to the BJAB cell nucleus (third row). Consistently, the fused cells remained viable more than 24 h after irradiation in all fusion experiments.

3. Discussion

Although gold nanoparticles are relatively chemically inert within biological tissue, they could strongly bind through various ligands to targeting molecules, thereby yielding simple, cost-effective, and stable conjugates of substantial binding specificity.[37,38] Their targeting efficiency could be further enhanced by using multiple targeting molecules,[39] resulting in an inherent ability to attach together cells that express different receptors, through strong chemical bonds. Once the cells are attached, the unique optical properties of the gold particles could be utilized to promote fusion. While the exact mechanism by which the irradiated nanoparticles promote cell fusion is as yet unclear, it is most likely triggered by the mechanical effect around the irradiated nanoparticles, which destabilizes the adjacent plasma membranes,[40] thus leading to the formation of a single hybrid cell with a unified cytoplasm. In our experiments, when the fluence of the femtosecond pulse train exceeded a certain threshold level (typically five pulses of 20 mJ cm^{-2} each), cells often underwent widespread necrosis, most likely due to their inability to effectively recover from the extensive membrane destabilization or rupture. Interestingly, cells that were undergoing fusion were less prone to necrosis than individual cells or unfused pairs of cells. A partial possible explanation for this observation is the lower surface area of the fusion product, which allows its plasma membrane to restore its integrity rapidly and more effectively. Another interesting observation was the mediating role of the BJAB cells in the fusion between two DCs, which resulted in the formation of numerous DC–DC–BJAB cell triplets. This property may potentially be used in various future applications to increase fusion efficiency between nonfusogenic cells.

Fusing different cells having different complementary properties into a single hybrid product of desired properties would be extremely valuable for various applications in tissue regeneration[41] and drug development,[42] and for the establishment of new therapeutic strategies.[43,44] In this proof-of-concept study, we have demonstrated specific fusion between tumor cells and DCs, the role of which in cancer vaccination is well characterized,[21] as well as fusion between tumor cells and macrophages, which are known to be involved in various immune regulation pathways;[45,46] the macrophages' exact role in stimulating antitumor response following fusion with cancer cells, however, is as yet unknown.

For specific applications, further research would be required for testing the functionality of the hybrid cell products. One potential obstacle for some applications would be the presence of remaining nanoparticles on the plasma membranes of the fusion products, which could interfere with their antigen presentation process. The remaining nanoparticles could also inhibit immune regulation processes that are

small 2013,
DOI: 10.1002/smll.201300696

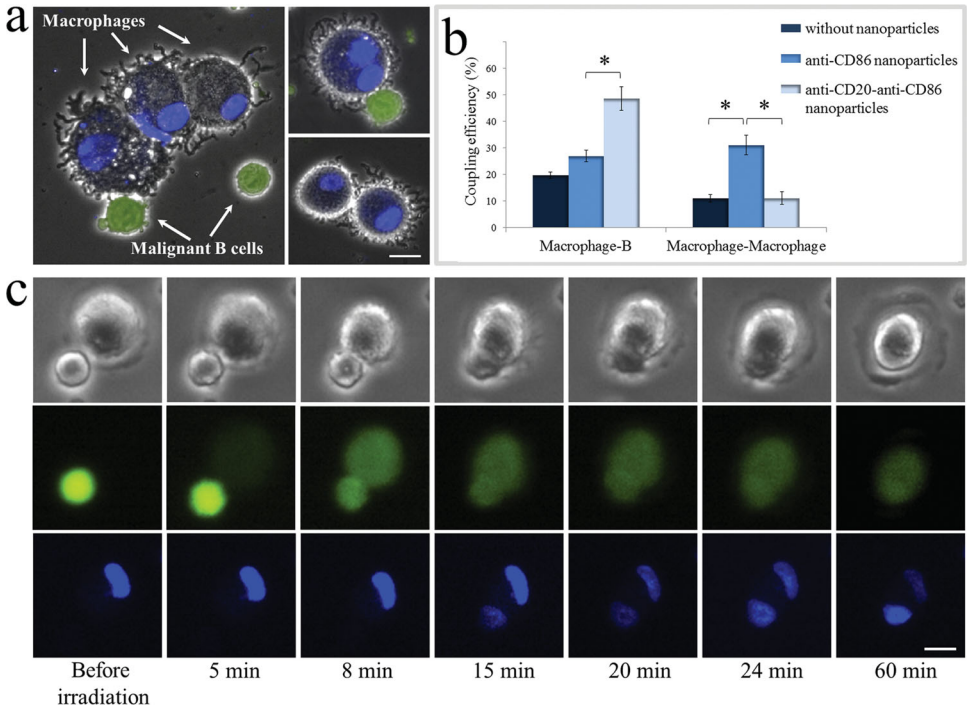

Figure 5. Macrophage–B cell coupling and fusion. a) Three selected regions of interest from a fluorescence-phase contrast image of macrophages (blue nuclei) and BJAB cells (green cytoplasm) after incubation with anti-CD20–anti-CD86 nanoparticles. Bar chart: Macrophage–BJAB and macrophage–macrophage attachment efficiency for different particles. (*) indicates $P<0.0001$. b) Time-lapse image sequence of fusing macrophage (top right) and BJAB (bottom left) cells following pulse irradiation. Phase contrast, green, and blue fluorescence images (top, middle, and bottom panels, respectively) show the redistribution of the cells' content during fusion. Scale bars represent 10 μm.

usually initiated via the conjugated receptors. One could avoid these difficulties by developing a method for nondestructive removal of the nanoparticles from the fusion products, or alternatively, by minimizing the total particle concentration during the course of the attachment–fusion process. Finally, antibody detachment from the gold nanoparticles could be harmful for various in vivo and ex vivo applications, due to undesired triggering of complement-dependent cytotoxicity.[47] The problem could be minimized by optimizing the antibody-to-particle ratio within the bispecific nanoparticles, thereby minimizing the amount of released antibodies.

4. Conclusion

In summary, we have presented a novel technique for selective fusion between antigen-presenting cells and tumor cells, by using specifically designed nanoparticles for the attachment of selected cells, and fusion of their plasma membranes following irradiation by a short sequence of resonant femtosecond laser pulses. The low toxicity of the gold particles, high specificity, efficiency, and relative simplicity of this approach would make it useful for a wide range of biomedical applications, and open new possibilities in biotechnology and in fundamental biological research. This approach would also broaden the use of nanotechnology for various biomedical applications by offering effective means for triggering and controlling desired interactions on a nanometer scale, potentially resulting in a more accurate research procedure and less invasive medical intervention.

5. Experimental Section

Cell Cultures: BJAB cells were grown at 37 °C and 5% CO_2 in RPMI-1640 medium (Sigma, Israel) supplemented with 2 mM glutamine, 5 mM sodium pyruvate, and 10% heat-inactivated fetal bovine serum. Cells were maintained at a concentration below 10^6 cells per mL to allow logarithmic growth.

Isolation and Differentiation of Dendritic Cells and Macrophages: Peripheral blood mononuclear cells from a consenting healthy donor were isolated by Lymphoprep (Axis Shield, Norway) density centrifugation according to the manufacturer's protocol, and cultured in RPMI-1640 with 5% autologous plasma for 1–2 h. Nonadherent cells were removed, and the adherent population was cultured for 5–7 days in RPMI-1640 containing only 5% autologous serum or RPMI-1640 containing 5% autologous serum, 500 units mL^{-1} recombinant human interleukin-4 (BioVision, USA), and 1000 units mL^{-1} granulocyte macrophage colony-stimulating factor (BioVision, USA), to yield macrophages and immature DCs, respectively. Half-volume medium replacement was performed every 3 days. DC maturation was obtained by adding 100 units mL^{-1} of tumor necrosis factor-α (BioVision, USA) to the medium at day 7.

Nanoparticle Preparation: Gold nanoparticles were prepared using a citrate reduction protocol[48] resulting in an average particle diameter of 25 nm. Anti-CD20 (Rituximab, Roche Israel) and anti-CD86 (BioLegend, USA) coating of gold nanoparticles was carried out according to Weiss et al.[49] with some modifications. Briefly, antibodies were incubated with OPSS-PEG2000-NHS (JenKem, USA) for 1 h in a mole ratio of 1:5000, followed by an additional 1 h of incubation with gold nanospheres in a mole ratio of $1:10^6$

DOI: 10.1002/smll.201300696

gold nanoparticles:OPSS-PEG2000-NHS. Glycine (30 mM) was added for overnight incubation followed by three washes with phosphate-buffered saline (PBS). Conjugation of both antibodies to the gold particles was confirmed by detaching the antibody coating layer from the gold nanospheres by using β-mercaptoethanol and analyzing the reduced solution using gel electrophoresis followed by Western blot analysis.

Scanning Electron Microscopy: Cells were fixed with 3% glutaraldehyde and mounted on polylysine-coated silicon chips (Ted Pella, Inc.). Samples were then fixed with 1% osmium and dehydrated as described elsewhere.[50] The microscope system used (Zeiss Ultra Plus HRSEM) was equipped with a Schottky field-emission electron gun and BalTec VCT100 cold stage maintained at –150 °C.

Specific Attachment and Fusion Experiments: BJAB cells were stained with 1 μM calcein acetoxymethyl ester for 15 min at room temperature, followed by three PBS washes. DCs and macrophage nuclei were stained with Hoechst 33342 (2 μg mL^{-1}; Sigma, Israel) for 15 min at room temperature followed by washes with PBS and 3 min of incubation with trypsin, in order to obtain nonadherent antigen-presenting cells (APCs). Cells were then mixed in a 1:1 ratio (APCs:BJAB cells) in the presence of antibody-coated gold nanoparticles (5×10^{10} particles mL^{-1}) for 20 min at room temperature under moderate shaking. Following incubation, the cells were washed three times with PBS and seeded on eight-well chamber slides (Lab-Tek II, Thermo Scientific). Pairs of APCs and BJAB cells were then counted based on the cells' morphology and fluorescent dyes. The statistical significance of the results was assessed based on counting at least 500 cells and using a two-proportion *z*-test.

Laser Pulse Irradiation: A beam from a Ti:sapphire oscillator (Tsunami, Spectra Physics) was amplified (Spitfire Pro XP, Spectra Physics) and wavelength-tuned to 545 nm by using an optical parametric amplifier (Topas-C, Spectra Physics). The pulse duration was 50 fs at a 1 kHz repetition rate. Cells were irradiated within eight-well chamber slides (Lab-Tek II, Thermo Scientific), which were placed within a microscope incubator (Okolab Inc.) at controlled temperature and CO_2 concentration. The irradiation pattern was a 35×35 rectangular array of 250-μm-diameter spots (approximately 75 mm^2 total area). Multiple pulse irradiation per spot was achieved by scanning the beam at lower rates, so that each point was irradiated by several consequent overlapping spots.

Acknowledgements

We thank Prof. Yoram Reiter and Dr. Gili Bisker for enlightening discussions, Prof. Doron Melamed for providing the Burkitt lymphoma cell line, and Dima Bourdetsky and Ravit Oren for technical assistance. This work was funded in part by a European Research Council starting grant (239986) and by the Lorry I. Lokey Interdisciplinary Center for Life Sciences and Engineering.

[1] G. P. Dunn, L. J. Old, R. D. Schreiber, *Immunity* **2004**, *21*, 137.
[2] E. J. Roy, U. Gawlick, B. A. Orr, D. M. Kranz, *Adv. Drug Delivery Rev.* **2004**, *56*, 1219.
[3] R. D. Jachimowicz, G. Fracasso, P. J. Yazaki, B. E. Power, P. Borchmann, A. Engert, H. P. Hansen, K. S. Reiners, M. Marie, E. P. von Strandmann, A. Rothe, *Mol. Cancer Ther.* **2011**, *10*, 1036.
[4] B. Karpovsky, J. A. Titus, D. A. Stephany, D. M. Segal, *J. Exp. Med.* **1984**, *160*, 1686.
[5] M. Brennan, P. F. Davison, H. Paulus, *Science* **1985**, *229*, 81.
[6] C. Milstein, A. C. Cuello, *Nature* **1983**, *305*, 537.
[7] U. D. Staerz, O. Kanagawa, M. J. Bevan, *Nature* **1985**, *314*, 628.
[8] P. Perez, R. W. Hoffman, S. Shaw, J. A. Bluestone, D. M. Segal, *Nature* **1985**, *316*, 354.
[9] P. K. Wallace, J. L. Romet-Lemonne, M. Chokri, L. H. Kasper, M. W. Fanger, C. E. Fadul, *Cancer Immunol. Immunother.* **2000**, *49*, 493.
[10] A. Hombach, W. Jung, C. Pohl, C. Renner, U. Sahin, R. Schmits, J. Wolf, U. Kapp, V. Diehl, M. Pfreundschuh, *Int. J. Cancer* **1993**, *55*, 830.
[11] S. Johnson, S. Burke, L. Huang, S. Gorlatov, H. Li, W. Wang, W. Zhang, N. Tuaillon, J. Rainey, B. Barat, Y. Yang, L. Jin, V. Ciccarone, P. A. Moore, S. Koenig, E. Bonvini, *J. Mol. Biol.* **2010**, *399*, 436.
[12] A. Loffler, P. Kufer, R. Lutterbuse, F. Zettl, P. T. Daniel, J. M. Schwenkenbecher, G. Riethmuller, B. Dorken, R. C. Bargou, *Blood* **2000**, *95*, 2098.
[13] P. A. Baeuerle, P. Kufer, R. Bargou, *Curr. Opin. Mol. Ther.* **2009**, *11*, 22.
[14] R. M. Steinman, *Annu. Rev. Immunol.* **1991**, *9*, 271.
[15] J. Gong, N. Nikrui, D. Chen, S. Koido, Z. Wu, Y. Tanaka, S. Cannistra, D. Avigan, D. Kufe, *J. Immunol.* **2000**, *165*, 1705.
[16] J. Gong, D. Avigan, D. Chen, Z. Wu, S. Koido, M. Kashiwaba, D. Kufe, *Proc. Natl. Acad. Sci. USA* **2000**, *97*, 2715.
[17] T. Kikuchi, Y. Akasaki, M. Irie, S. Homma, T. Abe, T. Ohno, *Cancer Immunol. Immunother.* **2001**, *50*, 337.
[18] J. Galea-Lauri, D. Darling, G. Mufti, P. Harrison, F. Farzaneh, *Cancer Immunol. Immunother.* **2002**, *51*, 299.
[19] N. Raje, T. Hideshima, F. E. Davies, D. Chauhan, S. P. Treon, G. Young, Y.-T. Tai, D. Avigan, J. Gong, R. L. Schlossman, P. Richardson, D. W. Kufe, K. C. Anderson, *Br. J. Haematol.* **2004**, *125*, 343.
[20] D. Avigan, B. Vasir, J. Gong, V. Borges, Z. Wu, L. Uhl, M. Atkins, J. Mier, D. McDermott, T. Smith, N. Giallambardo, C. Stone, K. Schadt, J. Dolgoff, J.-C. Tetreault, M. Villarroel, D. Kufe, *Clin. Cancer Res.* **2004**, *10*, 4699.
[21] D. Avigan, *Blood Rev.* **1999**, *13*, 51.
[22] S. Koido, M. Ohana, C. Liu, N. Nikrui, J. Durfee, A. Lerner, J. Gong, *Clin. Immunol.* **2004**, *113*, 261.
[23] J. Gong, D. Chen, M. Kashiwaba, D. Kufe, *Nat. Med.* **1997**, *3*, 558.
[24] S. Schneiderman, J. L. Farber, R. Baserga, *Somatic Cell Genet.* **1979**, *5*, 263.
[25] E. Gottfried, R. Krieg, C. Eichelberg, R. Andreesen, A. Mackensen, S. W. Krause, *Cancer Immun.* **2002**, *2*, 15.
[26] U. Zimmermann, *Biochim. Biophys. Acta* **1982**, *694*, 227.
[27] S. Nagata, K. Yamamoto, Y. Ueno, T. Kurata, J. Chiba, *Hybridoma* **1991**, *10*, 369.
[28] A. Vogel, J. Noack, G. Hüttman, G. Paltauf, *Appl. Phys. B: Lasers Opt.* **2005**, *81*, 1015.
[29] R. W. Steubing, S. Cheng, W. H. Wright, Y. Numajiri, M. W. Berns, *Cytometry* **1991**, *12*, 505.
[30] K. Kuetemeyer, A. Lucas-Hahn, B. Petersen, H. Niemann, A. Heisterkamp, *J. Biomed. Opt.* **2011**, *16*, 088001.
[31] T. F. Tedder, M. Streuli, S. F. Schlossman, H. Saito, *Proc. Natl. Acad. Sci. USA* **1988**, *85*, 208.
[32] J. W. Young, L. Koulova, S. A. Soergel, E. A. Clark, R. M. Steinman, B. Dupont, *J. Clin. Invest.* **1992**, *90*, 229.
[33] L. Minai, D. Yeheskely-Hayon, L. Golan, G. Bisker, E. J. Dann, D. Yelin, *Small* **2012**, *8*, 1732.
[34] A. N. Volkov, C. Sevilla, L. V. Zhigilei, *Appl. Surf. Sci.* **2007**, *253*, 6394.

DOI: 10.1002/smll.201300696

[35] G. Bisker, D. Yelin, *J. Opt. Soc. Am. B* **2012**, *29*, 1383.
[36] E. Lukianova-Hleb, Y. Hu, L. Latterini, L. Tarpani, S. Lee, R. A. Drezek, J. H. Hafner, D. O. Lapotko, *ACS Nano* **2010**, *4*, 2109.
[37] X. Cai, S. Conley, M. Naash, *Vision Res.* **2008**, *48*, 319.
[38] A. Llevot, D. Astruc, *Chem. Soc. Rev.* **2012**, *41*, 242.
[39] S. Bhattacharyya, J. A. Khan, G. L. Curran, J. D. Robertson, R. Bhattacharya, P. Mukherjee, *Adv. Mater.* **2011**, *23*, 5034.
[40] G. Wu, A. Mikhailovsky, H. A. Khant, C. Fu, W. Chiu, J. A. Zasadzinski, *J. Am. Chem. Soc.* **2008**, *130*, 8175.
[41] C. A. Cowan, J. Atienza, D. A. Melton, K. Eggan, *Science* **2005**, *309*, 1369.
[42] G. Kohler, C. Milstein, *Nature* **1975**, *256*, 495.
[43] Y. Guo, M. Wu, H. Chen, X. Wang, G. Liu, G. Li, J. Ma, M. S. Sy, *Science* **1994**, *263*, 518.
[44] K.-W. Peng, C. J. TenEyck, E. Galanis, K. R. Kalli, L. C. Hartmann, S. J. Russell, *Cancer Res.* **2002**, *62*, 4656.
[45] A. Mantovani, P. Allavena, A. Sica, *Eur. J. Cancer* **2004**, *40*, 1660.
[46] D. M. Mosser, J. P. Edwards, *Nat. Rev. Immunol.* **2008**, *8*, 958.
[47] G. Bisker, D. Yeheskely-Hayon, L. Minai, D. Yelin, *J. Controlled Release* **2012**, *162*, 303.
[48] J. Turkevich, P. C. Stevenson, J. Hillier, *J. Phys. Chem.* **1953**, *57*, 670.
[49] A. Weiss, T. C. Preston, J. Popov, Q. Li, S. Wu, K. C. Chou, H. M. Burt, M. B. Bally, R. Signorell, *J. Phys. Chem. C* **2009**, *113*, 20252.
[50] L. Shaulov, R. Gruber, I. Cohen, A. Harel, *J. Cell Sci.* **2011**, *124*, 3822.

Received: March 5, 2013
Revised: April 15, 2013
Published online: